Bias-Corrected and Dynamically-Downscaled Hourly Temperature Projections for Sea-Tac

Guillaume Mauger and Jason Won

University of Washington Climate Impacts Group

Dec 2021

TABLE OF CONTENTS

CITATION: Mauger, G.S. and J.S. Won. 2021. Bias-Corrected and Dynamically-Downscaled Hourly Temperature Projections for Sea-Tac. Report prepared for Seattle City Light. Climate Impacts Group, University of Washington.

ACKNOWLEDGEMENT: This work was funded via a grant from Seattle City Light.

Purpose

Load forecasting requires hourly temperature estimates in order to better estimate energy demand. This memo describes the bias-correction approach used to develop new dynamically-downscaled projections of historical and future hourly temperatures at Sea-Tac. The purpose of this memo is two-fold:

1. Describe the general approach to bias correcting all WRF hourly temperatures, and
2. Describe the additional bias-correction applied to correct for anomalous cold snaps.

Background

In an ongoing project funded by Seattle City Light (SCL), we are using new dynamically-downscaled projections to estimate changes in extreme winds, temperature, and lightning. The dynamically-downscaled projections are based on results from the Weather Research and Forecasting community mesoscale model (WRF, http://www.wrf-model.org; Skamarock et al., 2008). We are using the WRF projections because they are expected to provide more accurate estimates of extreme events (e.g., Salathé et al. 2014). Nonetheless, the WRF simulations have biases relative to observed conditions.

In addition to more general biases for all times and conditions, we recently identified a bias in annual minimum temperature estimates from the WRF regional climate model. Subsequent analysis revealed that this bias originates in the Global Climate Models (GCMs) that provide the boundary conditions to the WRF simulations. Due to their coarse resolution, GCMs do not adequately represent the topography of the region. As a result, they allow cold continental air to flow into Puget Sound when in reality it would remain confined east of the Cascade and Rocky Mountains.

This memo describes the approach used to bias-correct the WRF hourly temperature projections at Sea-Tac.

Observed Data

SCL staff originally provided data from the NOAA Cooperative Observer program (COOP) station at Sea-Tac, with observations starting in 1970 and continuing to the present. However, this data only provided daily resolution data, which our tests indicated would not be adequate to bias-correct the WRF simulations. Specifically, we found different biases for daily minimum and maximum temperatures, indicating that a bias correction based on daily values would be inadequate.

Instead, we obtained hourly observations from the NOAA Integrated Surface Database (ISD, station ID: 72793024233). Measurements are taken from the same location as the COOP station used by SCL, but provide hourly temperature observations. In addition, we analyze the full record of available observations (1948-present) in order to maximize the sample size in order to improve the bias correction, particularly for extreme events. Although this involves using data from well before the 1970 start date for the WRF simulations, we expect the climate change trend to be small compared to the WRF biases we are correcting.

Model Data

Global Climate Model (GCM) Projections

GCM projections were obtained from the Climate Model Inter-comparison Project, phase 5 (CMIP5; Taylor et al., 2012). The GCMs included in the WRF ensemble (Table 1) were chosen based on Brewer et al. (2016), who evaluated and ranked global climate models based on their ability to reproduce the climate of the Pacific Northwest. All of the new projections are based on the high-end RCP 8.5 scenario (Van Vuuren et al., 2011).

Additional information on model evaluation and ranking is summarized in Mauger et al. (2019). In addition, Mauger et al. (2019) discuss approaches for using RCP 8.5 projections as an analog for what might be projected for the RCP 4.5 scenario. For example, the 2080s in the RCP 4.5 projections appear to correspond approximately to the 2040s or 2050s in the RCP 8.5 projections.

Regional Climate Model (WRF)

Regional Climate Model simulations were produced using the Weather Research and Forecasting (WRF, http://www.wrf-model.org; Skamarock et al., 2005) community mesoscale model, following the configuration developed in previous work (e.g., Salathé et al., 2010). The model, and model configuration, are described in detail in Lorente-Plazas et al. (2018) and Mauger et al. (2018).

The new ensemble of WRF projections includes one simulation for each of the GCMs listed in Table 1, in addition to the RCP 4.5 projection developed previously for the ACCESS 1.0 GCM. All simulations run from 1970-2099 and are archived at a 1-hour time step and a spatial resolution of 12 km.

Table 1. The twelve global climate models (GCMs) used as input to the regional model simulations. All simulations are based on the high-end RCP 8.5 greenhouse gas scenario (Van Vuuren et al., 2011). A low-end scenario was also produced for the ACCESS 1.0 model, resulting in two separate projections for this GCM.

Model	Center	Resolution	Vertical Levels
ACCESS1-0	Commonwealth Scientific and Industrial Research Organization (CSIRO), Australia/ Bureau of Meteorology, Australia	1.25 x 1.88	38
ACCESS1-3	Commonwealth Scientific and Industrial Research Organization (CSIRO), Australia/ Bureau of Meteorology, Australia	1.25 x 1.88	38
bcc-csm1-1	Beijing Climate Center (BCC), China Meteorological Administration	2.8 × 2.8	26
CanESM2	Canadian Centre for Climate Modeling and Analysis	2.8 × 2.8	35
CCSM4	National Center of Atmospheric Research (NCAR), USA	1.25 × 0.94	26
CSIRO-Mk3-6-0	Commonwealth Scientific and Industrial Research Organization (CSIRO) / Queensland Climate Change Centre of Excellence, Australia	1.8 × 1.8	18
FGOALS-g2	LASG, Institute of Atmospheric Physics, Chinese Academy of Sciences	2.8 × 2.8	26
GFDL-CM3	NOAA Geophysical Fluid Dynamics Laboratory, USA	2.5 × 2.0	48
GISS-E2-H	NASA Goddard Institute for Space Studies, USA	2.5 × 2.0	40
MIROC5	Atmosphere and Ocean Research Institute (The University of Tokyo), National Institute for Environmental Studies, and Japan Agency for Marine-Earth Science and Technology	1.4 × 1.4	40
MRI-CGCM3	Meteorological Research Institute, Japan	1.1 × 1.1	48
NorESM1-M	Norwegian Climate Center, Norway	2.5 × 1.9	26

Results

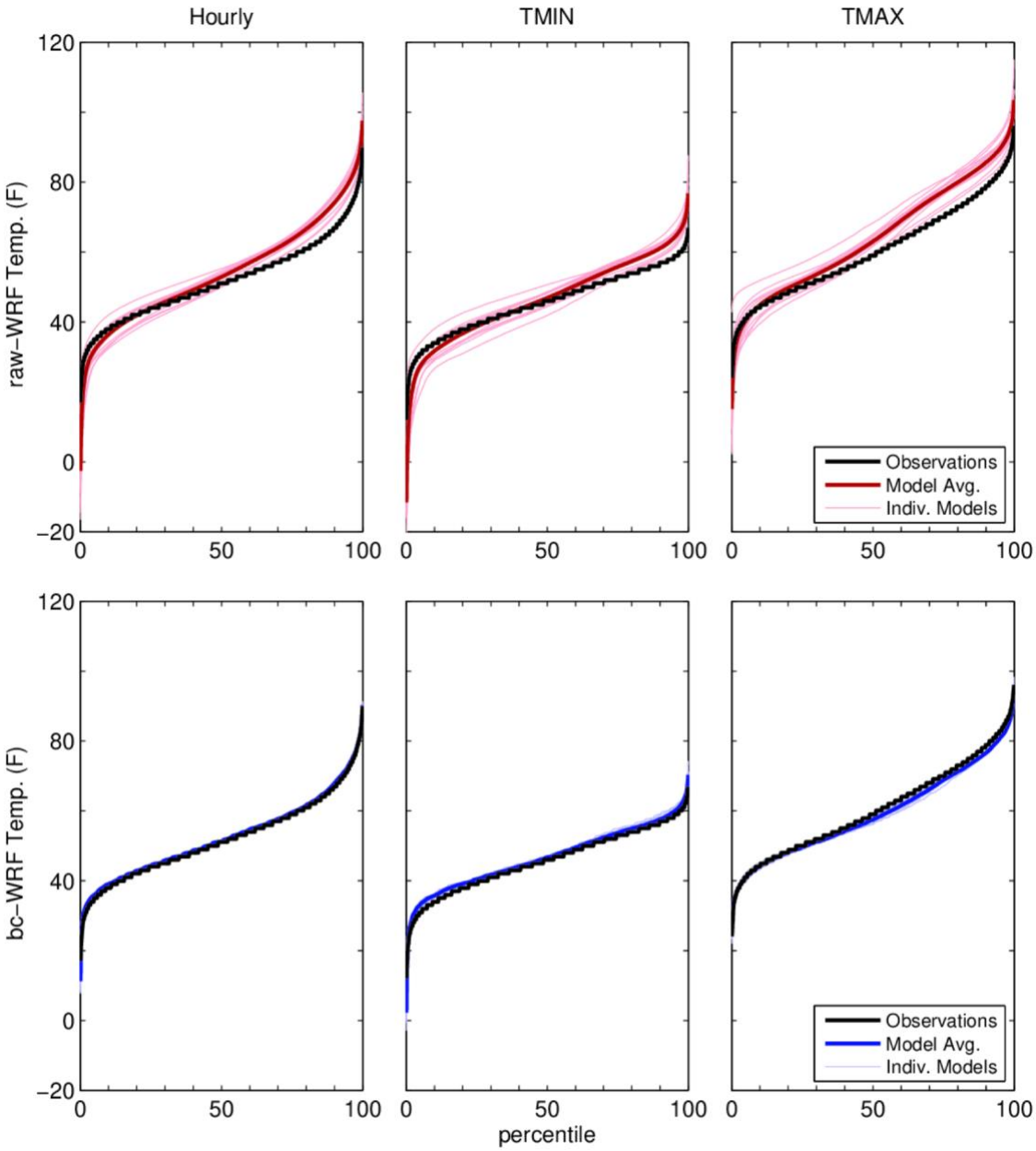

Figure 1. Cumulative distribution functions (CDFs) for observed vs un-corrected ("raw", top) WRF and bias-corrected WRF (bottom) temperature estimates. In order to better resolve biases in the extremes, results are displayed in increments of 0.1 percentile (0.1, 0.2, … 99.9%). The model average results (average of the 12 RCP 8.5 models) are shown with the thick red and blue lines, respectively; individual model results are shown with the lighter-colored thin lines. The raw WRF biases are not the same for daily minimum and maximum temperatures, meaning that the bias-correction must be applied via comparison with the hourly observations.

We compared both the daily and hourly temperature observations against WRF in order to decide which to use for the bias correction. Since the GCMs are "free running" simulations their time series do not match the timing of events. As a result, time series comparisons or scatter plots are not useful for evaluating model skill. Instead, we compare the cumulative distribution in hourly, daily minimum, and daily maximum temperatures for the uncorrected ("raw") WRF simulations vs the observations (Figure 1). We computed the empirical cumulative distribution function (CDF) using the standard approach of ranking all temperature values then estimating the quantile associated with each rank. The average CDF for all 12 RCP 8.5 model simulations is shown in addition to the results for each individual model. Results are shown for the full time series in the observations (1948-2020 for the hourly data, and 1970-2020 for the daily data), and for 1970-2020 for WRF.

Figure 1 makes it clear that a simple scaling cannot correct all WRF temperature biases. Specifically, we see that the WRF temperatures are biased high for high temperatures and low for low temperatures – the range in temperatures is too large. As noted above, the low temperature biases are particularly large, much larger than other biases. Specifically: the lowest WRF temperatures extend below 0ºF, whereas the lowest observed temperatures at Sea-Tac are between 10-20ºF. This means that a quantile-based bias correction will be needed to correct the WRF simulations.

Another question is if the daily observations can be used in the bias correction instead of the hourly data. In an initial analysis, not shown here, we confirmed that the hourly observations could be used to reproduce the daily maximum and minimum temperatures within a high degree of precision, so that we can be certain that differences in the comparisons are indeed a reflection of different biases in WRF. Having confirmed that the observations are internally consistent, Figure 1 shows that the WRF biases for daily minimum and maximum temperatures are not the same. This means that an hourly bias correction is needed.

In previous work we have shown that quantile-based bias-corrections can lead to spurious trends, especially for extreme events (Mauger et al. 2016). As part of that work, we developed a quantile-based approach that minimizes the influence of the tails of the distribution. In this approach we first binned the results separately for each quantile (0-1, 1-2, … 99-100), obtaining average values for each quantile, both for the observations and each model simulation. As above we compared the full record of observations with results from 1971-2020 in the WRF simulations. We then used the difference between the model and observed averages for each quantile to estimate a scaling. Each quantile scaling was then applied to all WRF time steps falling within each quantile. This process was repeated separately for each model.

After reviewing the results from the quantile-based bias correction, we saw that there remained large biases in the coldest events of each year. Specifically, in analyzing the observational record we find that the coldest events were never more than 35ºF colder than the Dec-Feb average temperature for that year. In contrast, the bias-corrected WRF results retained numerous events that were much colder than this. This cold snap bias is particularly problematic because climate change alters the frequency with which these weather events occur. Although such changes in weather events are expected and likely a real consequence of climate change, this led to exaggerated changes in the coldest winter temperatures because the temperatures are so anomalously cold when they do occur. By seeing less of those in the future, WRF was sometimes projecting changes of several degrees per decade for the coldest winter temperatures – about a factor of ten more than annual average changes in temperature.

We tested two different approaches to correcting for these anomalous cold snaps in the WRF results:

1. Quantile-based, where we further corrected all temperature values below a particular quantile (e.g.: 0.1%)
2. Event-based, where we identified anomalous cold snaps and corrected the temperature values for these events.

Although the event-based approach can consistently remove all cold snaps, there were two challenges with this approach. First, it requires a subjective definition of what constitutes an "anomalous" cold snap, when in fact it is likely that all cold events are biased, even when within the range of the observations. Second, once an event has been identified it is not clear what correction to apply. As a result we used a quantile-based correction in which we applied a scaling to all values below the 0.01% percentile. This essentially replicates the first bias-correction step, but is focused on the coldest temperatures.

In order to better illustrate the biases in the raw and bias-corrected WRF data – particularly the anomalous cold snaps – Figure 2 shows the difference between the observed and model CDF for each quantile. These show the vast improvement between the raw and bias-corrected results. In addition, we see that the anomalous cold snaps are not fully addressed in the bias-corrected results. Given the potential importance of the cold snaps for load forecasting, Appendix A includes plots of the raw and bias-corrected time series in the annual minimum temperature for each model. This is one indicator of the presence or absence of the anomalous cold snaps, which could lead to anomalous results in the load projections.

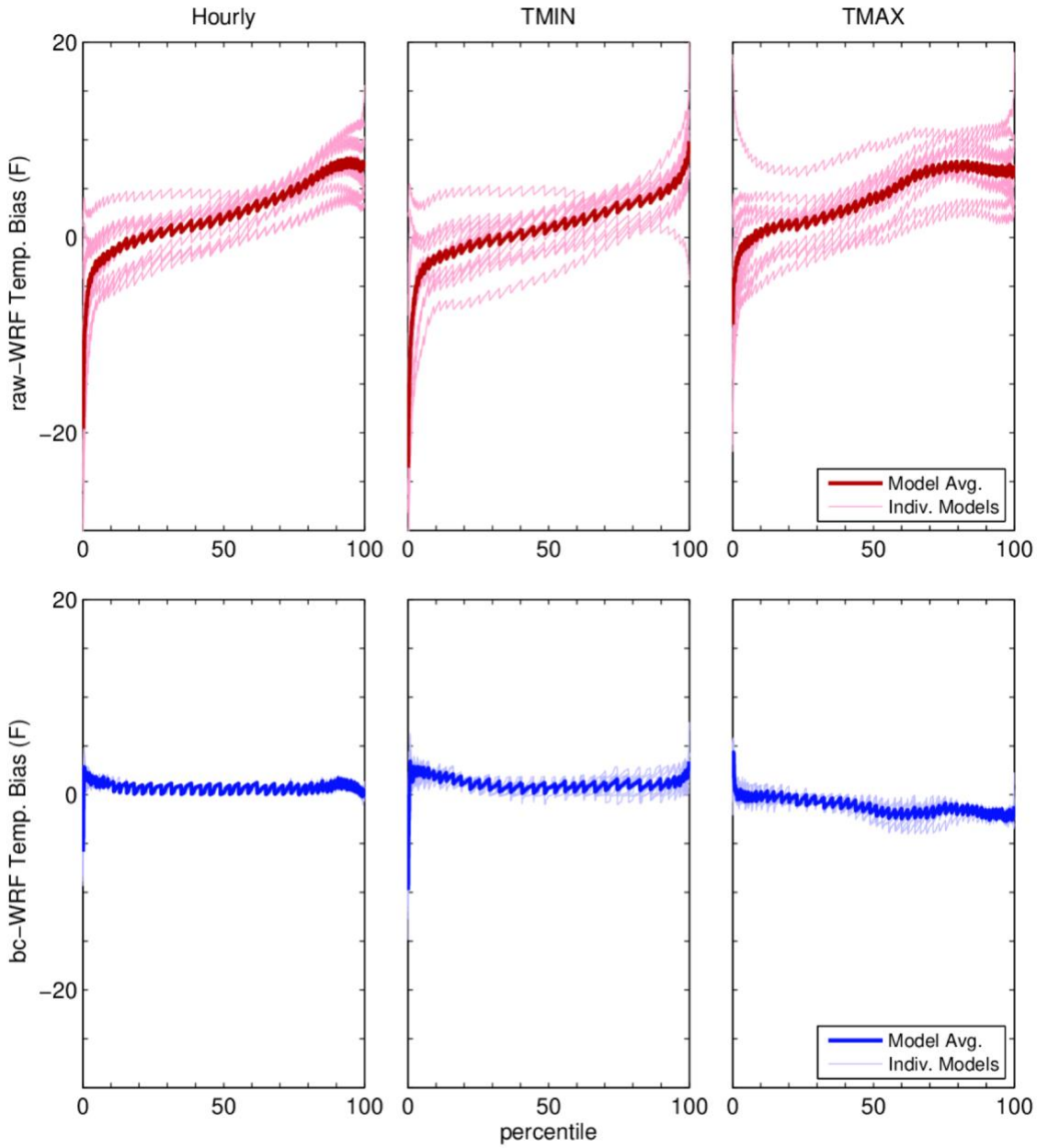

Figure 2. As in Figure 1 except showing the difference between the observations and each model for each quantile (WRF – observations, in ºF). The observations are discretized in 0.1 ºC increments, leading to the jagged pattern that can be seen in the difference plots. As discussed in the text, biases in the coldest events remain even in the bias-corrected results.

Discussion

Our cold snap bias correction is a very simplistic approach and could be improved with additional work. One avenue that we suggest exploring is to explore how to relate observed cold snaps at Sea-Tac with the large-scale conditions that drive them (e.g., surface pressure difference between Sea-Tac and Spokane). This would require isolating cold-snap events; one challenge with this approach would be to introduce corrections seemlessly in a way that doesn't alter other aspects of the WRF time series. A simpler approach could be to simply apply a more detailed bias-correction that is focused specifically on the coldest events. As noted above, quantile approaches need to be evaluated carefully to ensure that they do not introduce spurious trends.

One of the challenges associated with using alternative datasets, such as WRF, is that the load forecasting model is calibrated for a particular set of inputs, and that no dataset is going to replicate its statistics perfectly. As a result, we recommend also exploring approaches that involve perturbing the observed record used as input to the load forecasting model. This could be done in a variety of ways, but one approach could be to use a quantile-based scaling, similar to that used in the first bias-correction step described above.

References

Brewer, M. C., & Mass, C. F. (2016). Projected changes in western US large-scale summer synoptic circulations and variability in CMIP5 models. Journal of Climate, 29(16), 5965-5978

Lorente-Plazas, R., Mitchell, T.P., Mauger, G., Salathé, E.P., 2018. Local Enhancement of Extreme Precipitation during Atmospheric Rivers as Simulated in a Regional Climate Model. American Meteorological Society, 19:1429-1446. https://doi.org/10.1175/JHM-D-17-0246.1

Mauger, G.S., J.S. Won, 2019. Expanding the ensemble of precipitation projections for King County. Report prepared for the King County Department of Natural Resources. Climate Impacts Group, University of Washington, Seattle.

Mauger, G.S., S.-Y. Lee, C. Bandaragoda, Y. Serra, J.S. Won, 2016. Refined Estimates of Climate Change Affected Hydrology in the Chehalis basin. Report prepared for Anchor QEA, LLC. Climate Impacts Group, University of Washington, Seattle. doi:10.7915/CIG53F4MH

Salathé, E.P., Leung, L.R., Qian, Y., Zhang, Y. 2010. Regional climate model projections for the State of Washington. Climatic Change 102(1-2): 51-75, doi: 10.1007/s10584-010-9849-y.

Salathé Jr, E. P., Hamlet, A. F., Mass, C. F., Lee, S. Y., Stumbaugh, M., & Steed, R. (2014). Estimates of twenty-first-century flood risk in the Pacific Northwest based on regional climate model simulations. Journal of Hydrometeorology, 15(5), 1881-1899.

Skamarock, W. C., Klemp, J. B., Dudhia, J., Gill, D. O., Barker, D. M., Wang, W., & Powers, J. G. (2005). A description of the advanced research WRF version 2 (No. NCAR/TN-468+ STR). National Center for Atmospheric Research Boulder Co Mesoscale and Microscale Meteorology Div.

Taylor, K. E., Stouffer, R. J., & Meehl, G. A. (2012). An overview of CMIP5 and the experiment design. Bulletin of the American Meteorological Society, 93(4), 485-498.

Van Vuuren, D., J. Edmonds, M. Kainuma, K. Riahi, A. Thomson, K. Hibbard, G. Hurtt, T. Kram, V. Krey, J. Lamarque, T. Masui, M. Meinshausen, N. Nakicenovic, S. Smith, S. Rose, 2011: The representative concentration pathways: an overview. Climatic Change, 109: 5-31. http://dx.doi.org/10.1007/s10584-011-0148-z

Appendix A – Annual Minimum Temperature Plots

The figures below show the time series for the annual minimum in hourly temperatures, for each of the WRF simulations listed in Table 1. Results are shown for both uncorrected ("raw") and bias-corrected WRF results for each model. In some cases, the bias-corrected temperatures appear to saturate. This is a result of the bias-correction approach, which adjust temperatures to a fixed value that is 35ºF lower than the Dec-Feb average for each year.

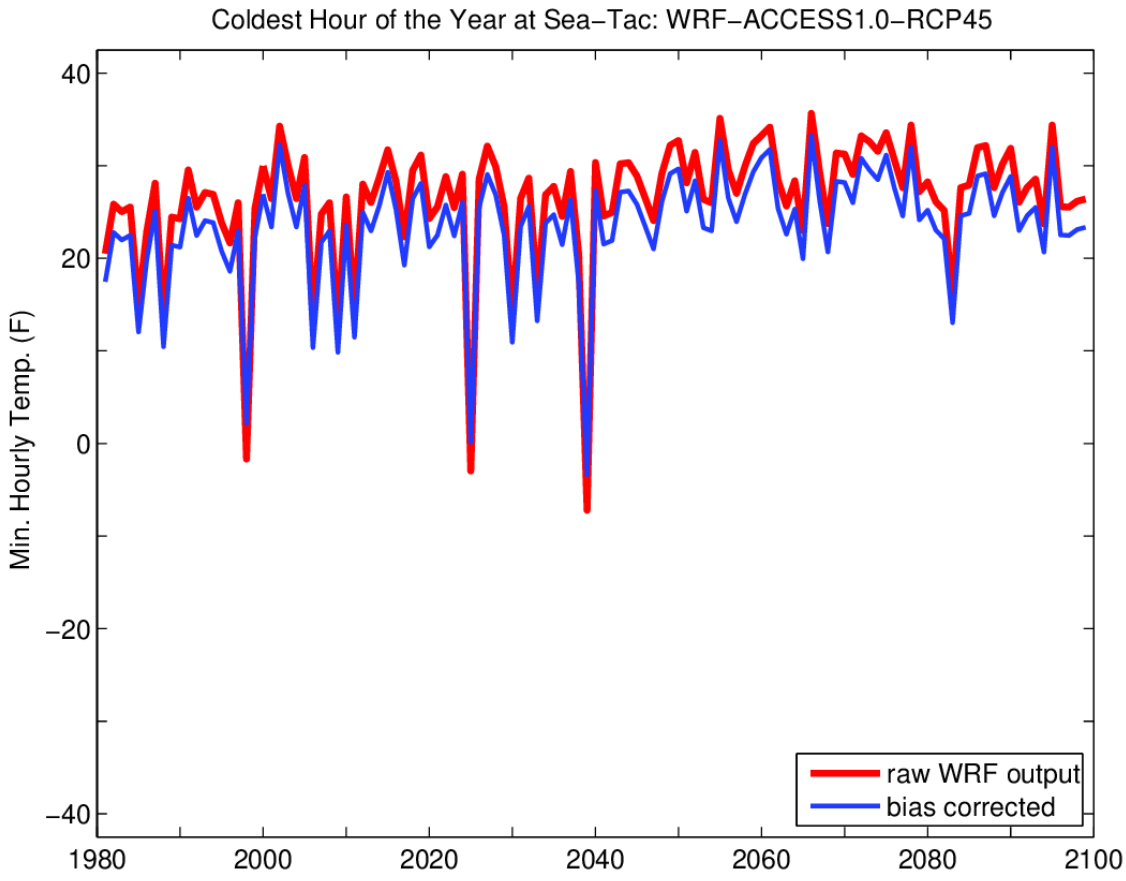

Figure A1. Time series of annual minimum temperature for ACCESS 1.0, RCP 4.5.

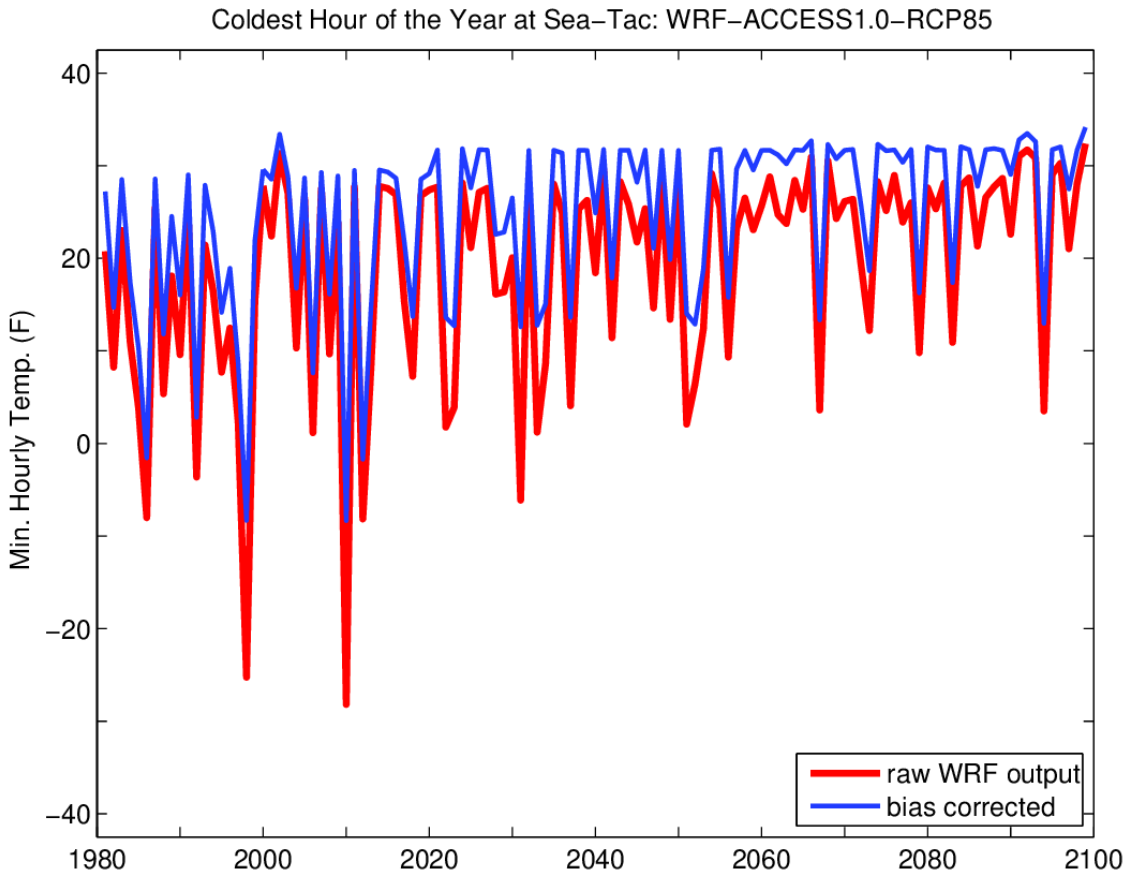

Figure A2. Time series of annual minimum temperature for ACCESS 1.0, RCP 8.5.

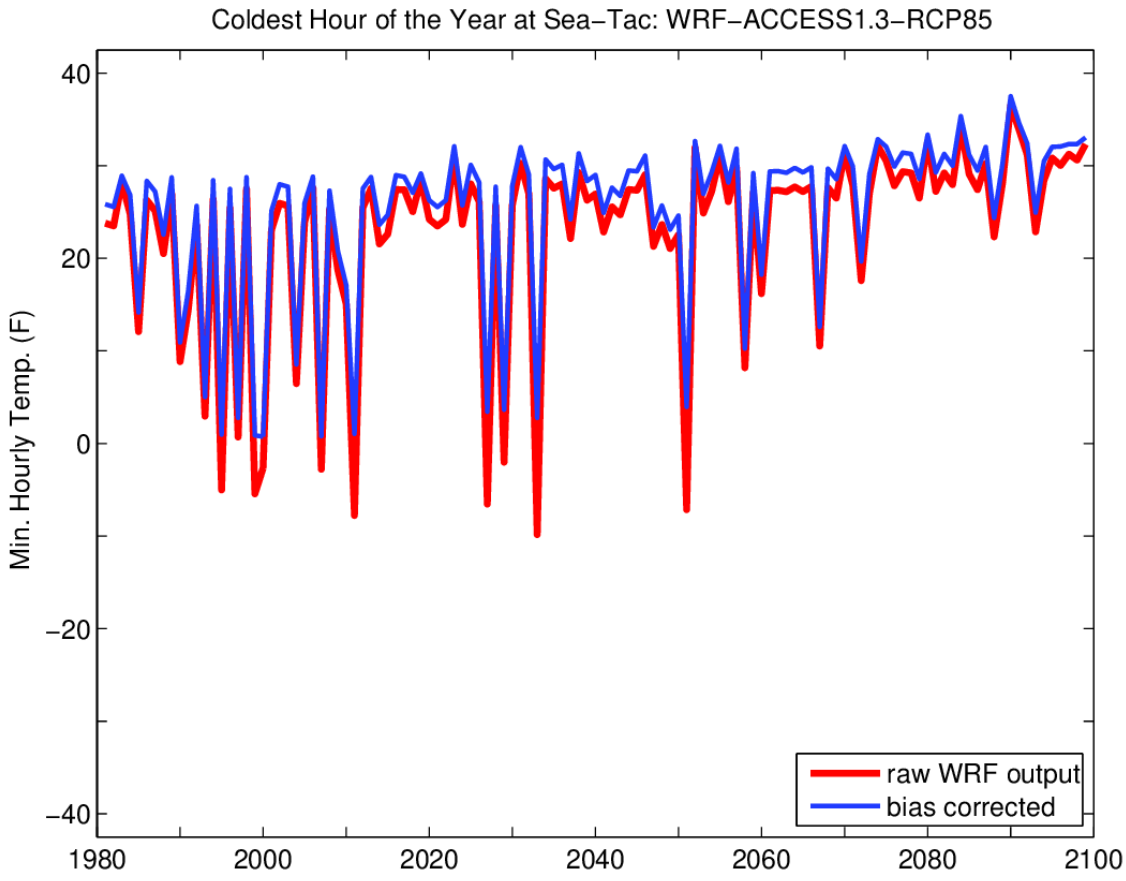

Figure A3. Time series of annual minimum temperature for ACCESS 1.3, RCP 8.5.

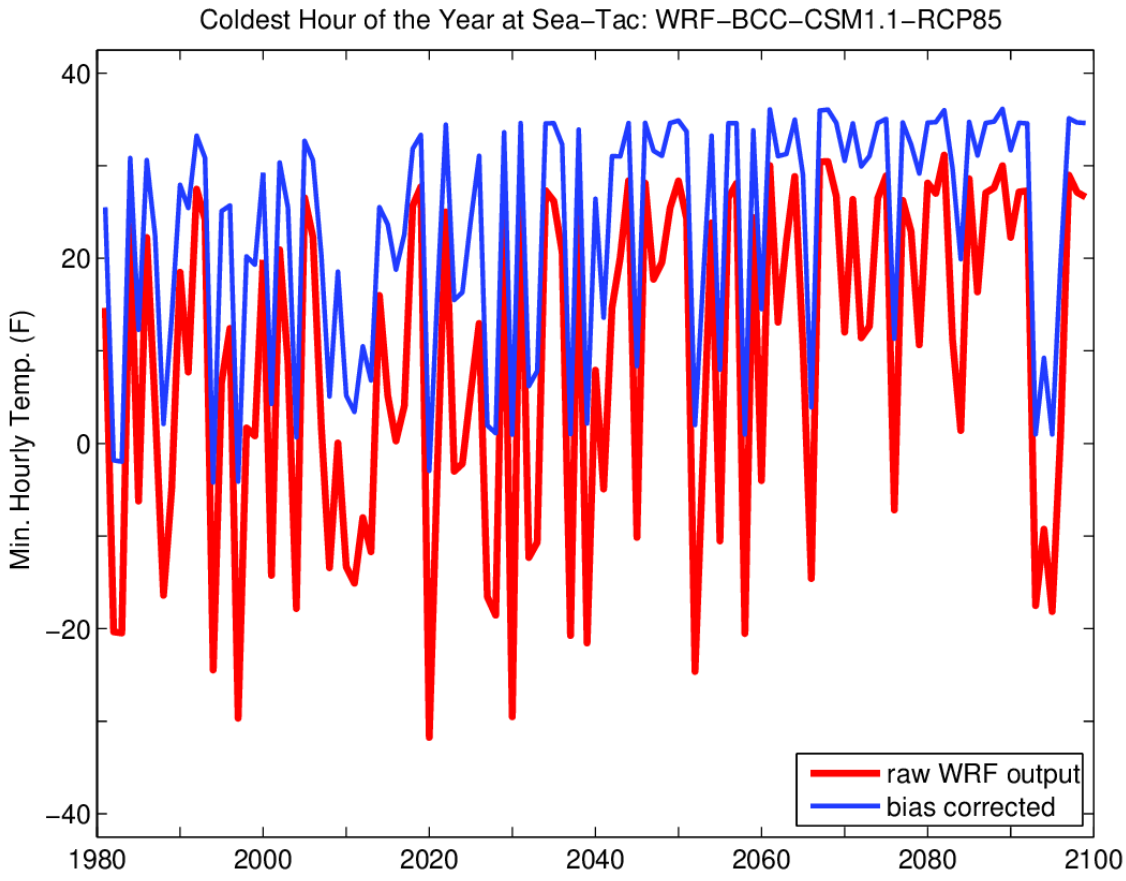

Figure A4. Time series of annual minimum temperature for BCC CSM 1.1, RCP 8.5.

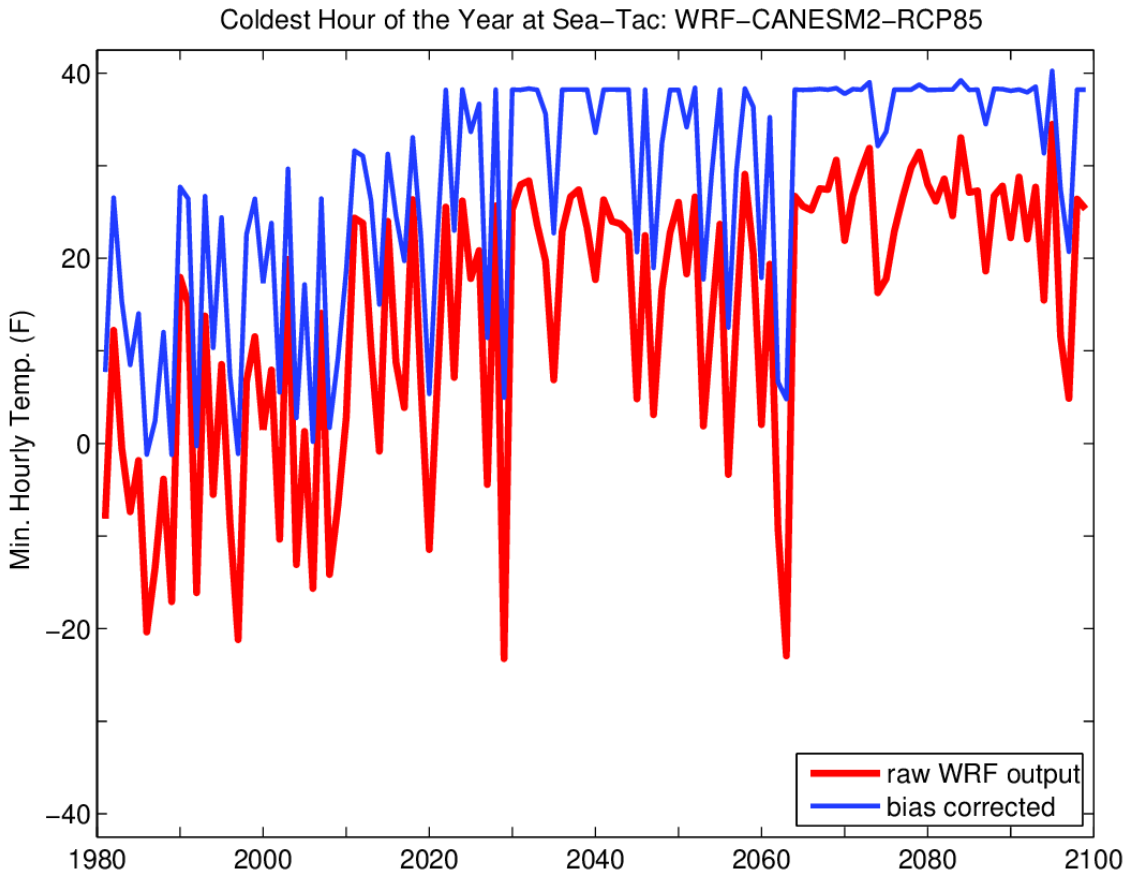

Figure A5. Time series of annual minimum temperature for CanESM2, RCP 8.5.

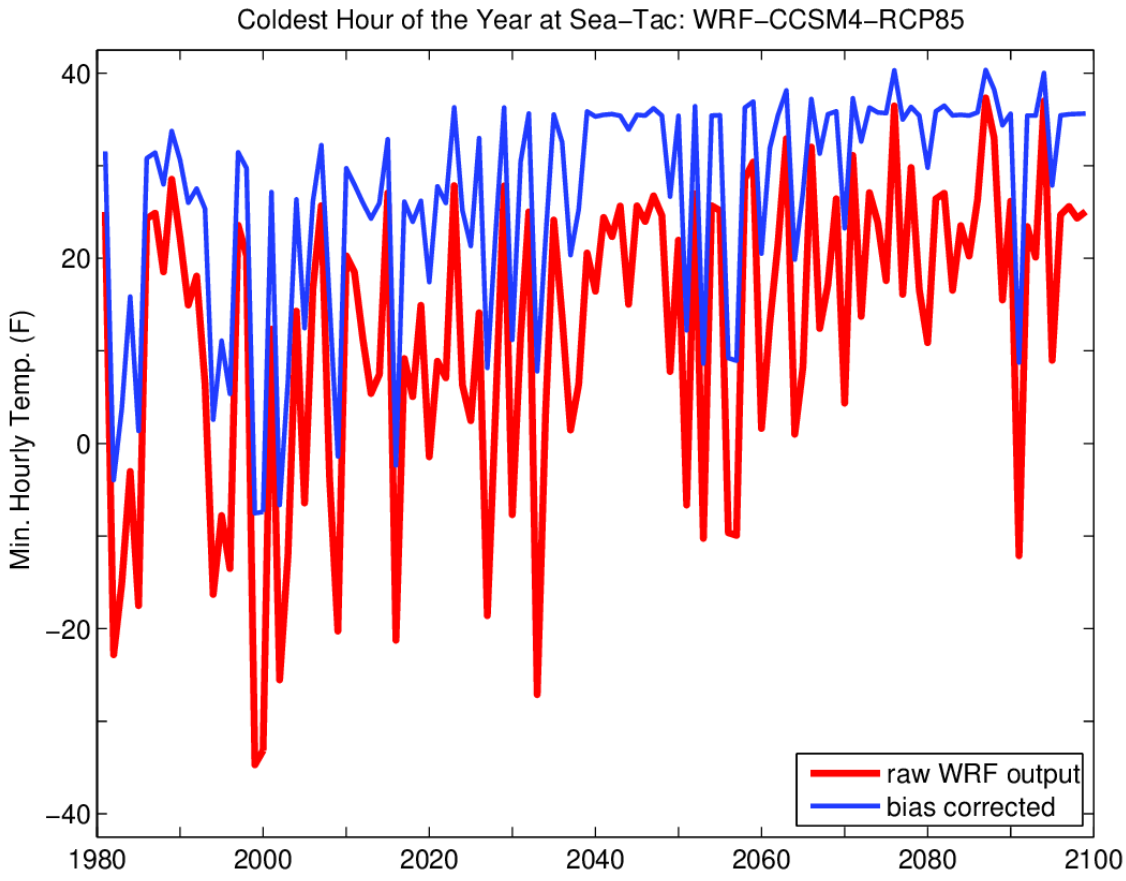

Figure A6. Time series of annual minimum temperature for CCSM4, RCP 8.5.

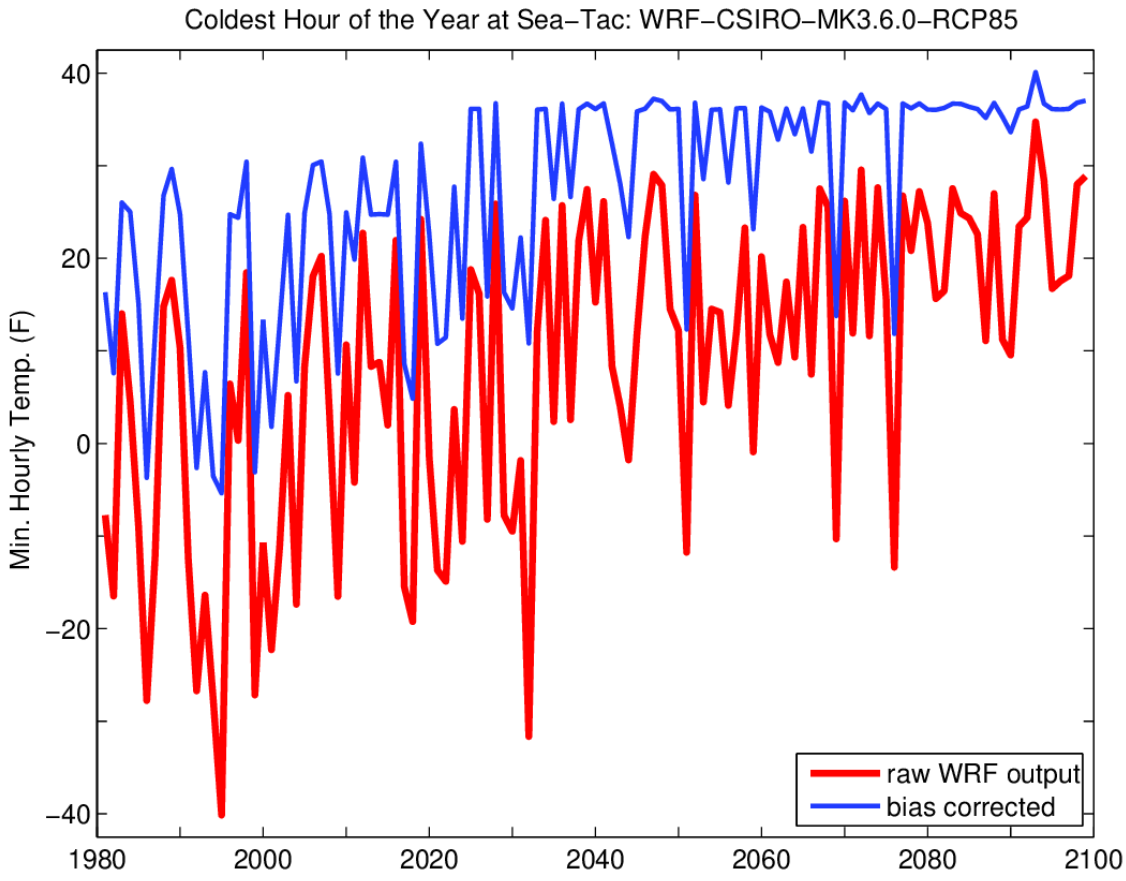

Figure A7. Time series of annual minimum temperature for CSIRO MK3.6.0, RCP 8.5.

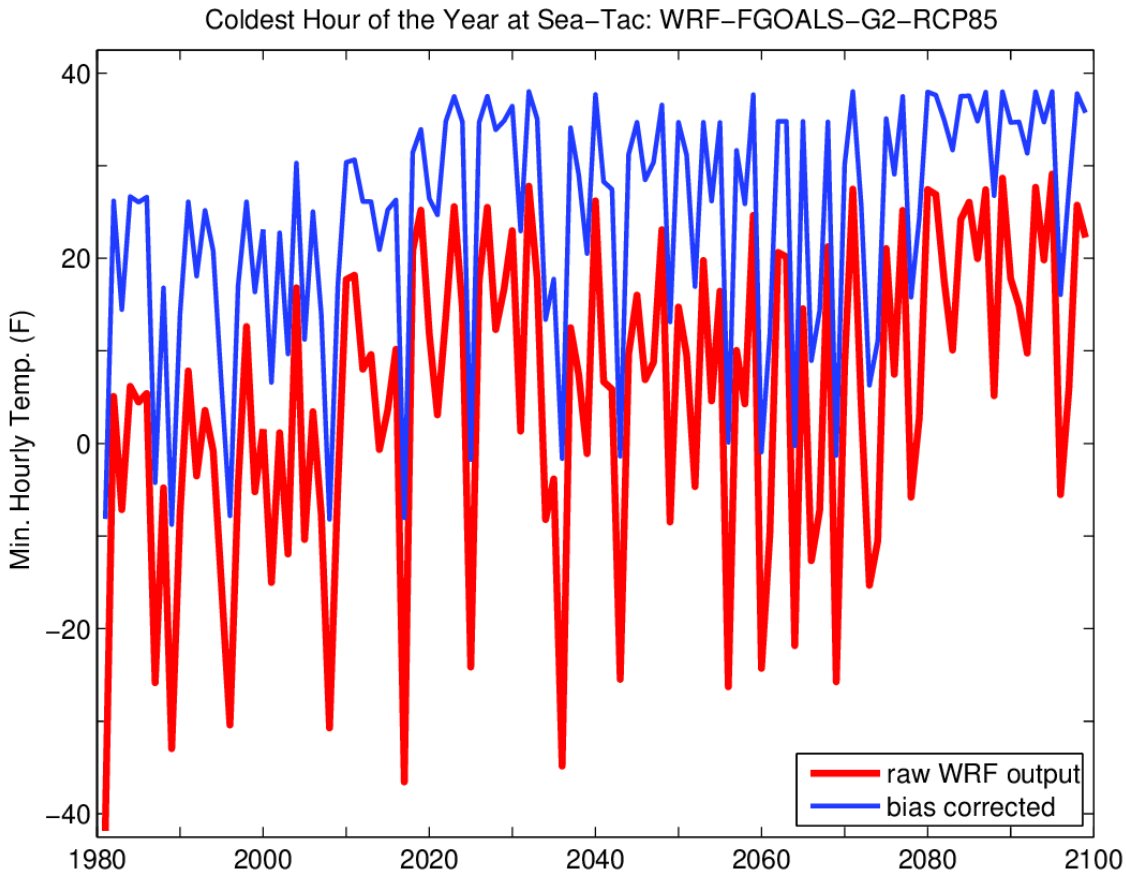

Figure A8. Time series of annual minimum temperature for FGOALS G2, RCP 8.5.

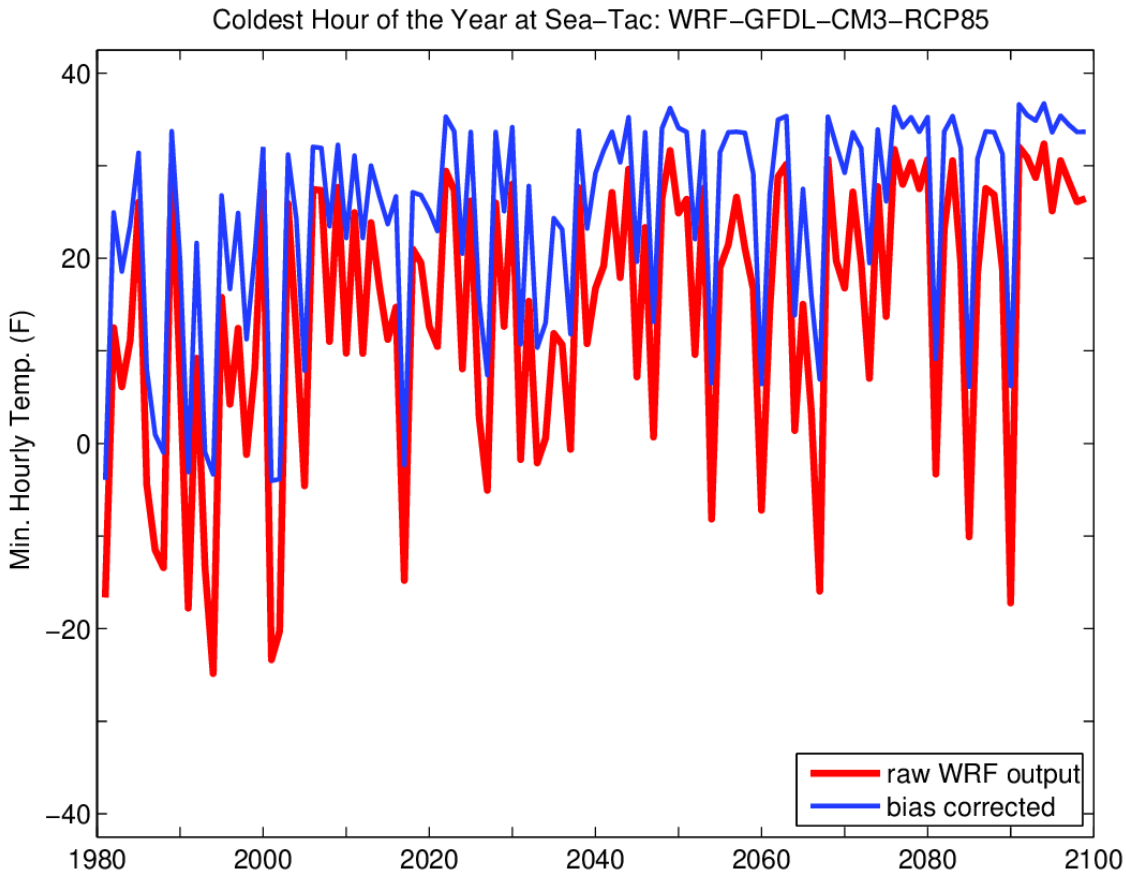

Figure A9. Time series of annual minimum temperature for GFDL CM3, RCP 8.5.

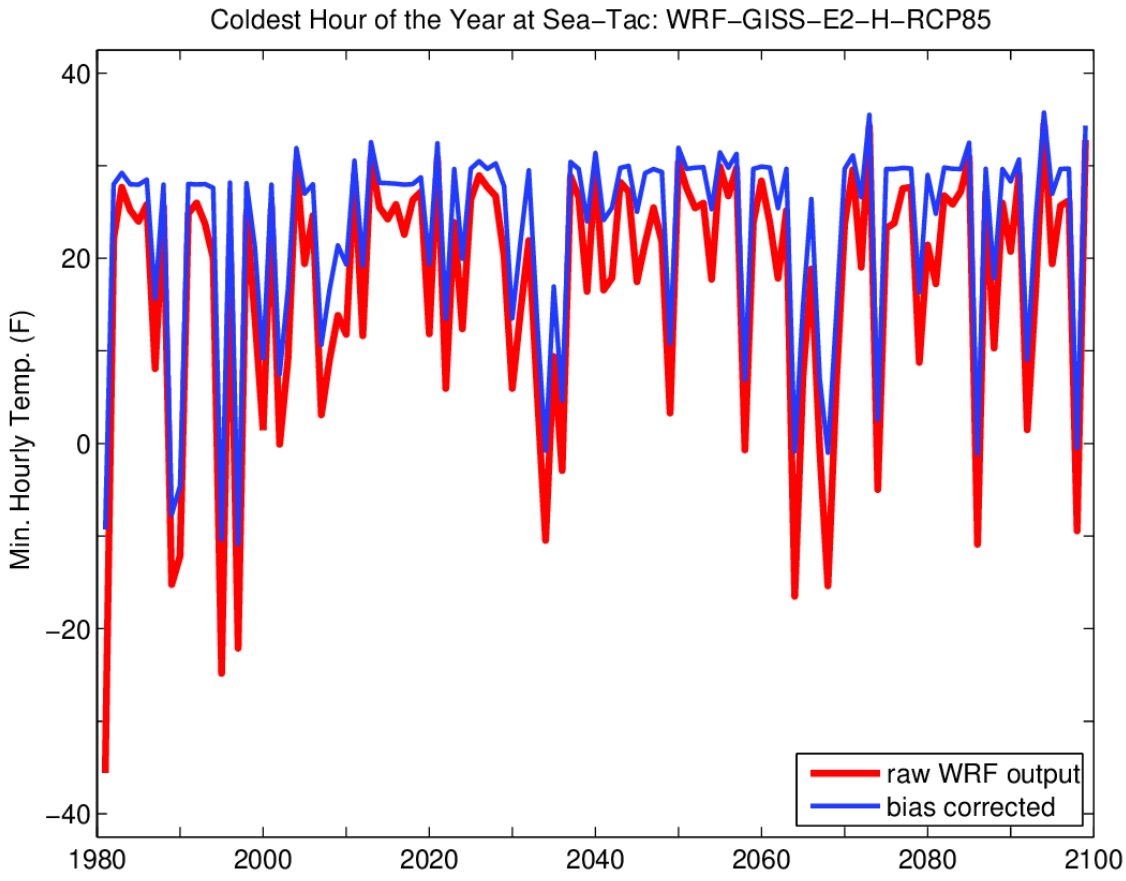

Figure A10. Time series of annual minimum temperature for GISS E2-H, RCP 8.5.

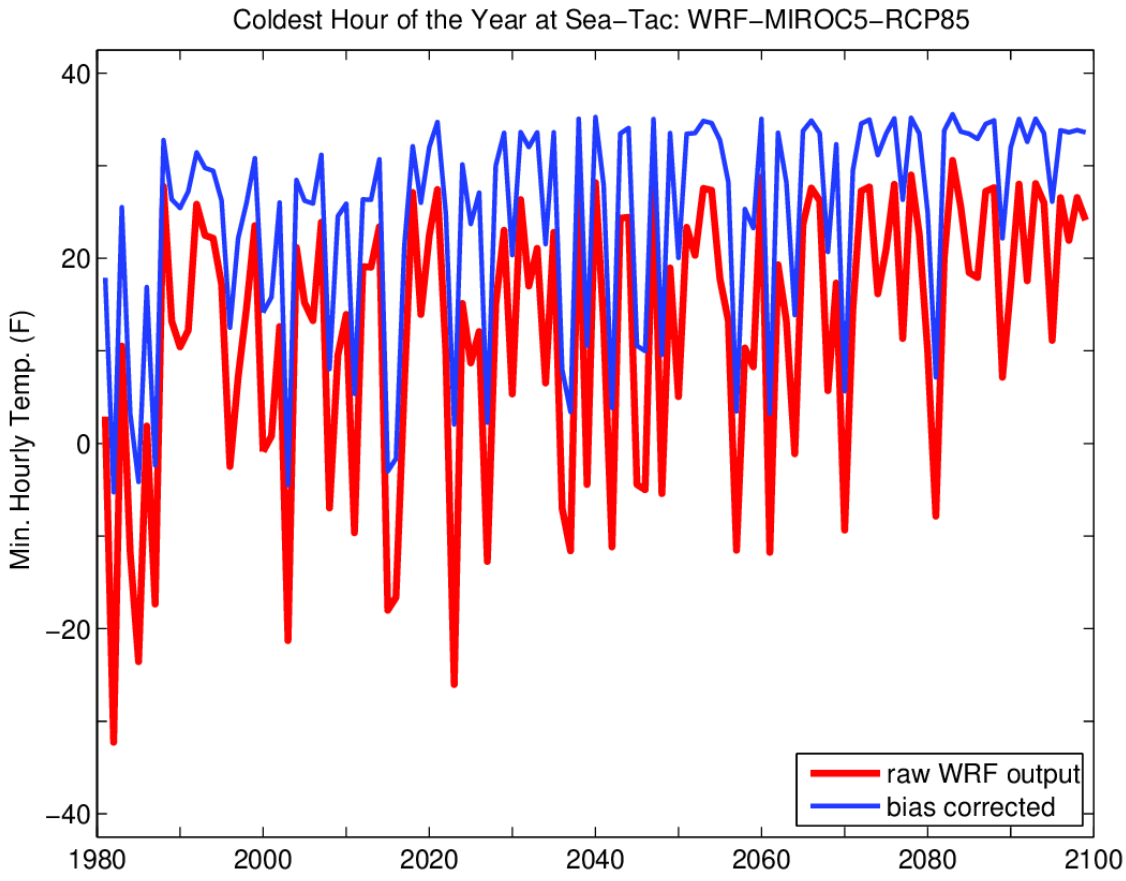

Figure A11. Time series of annual minimum temperature for MIROC5, RCP 8.5.

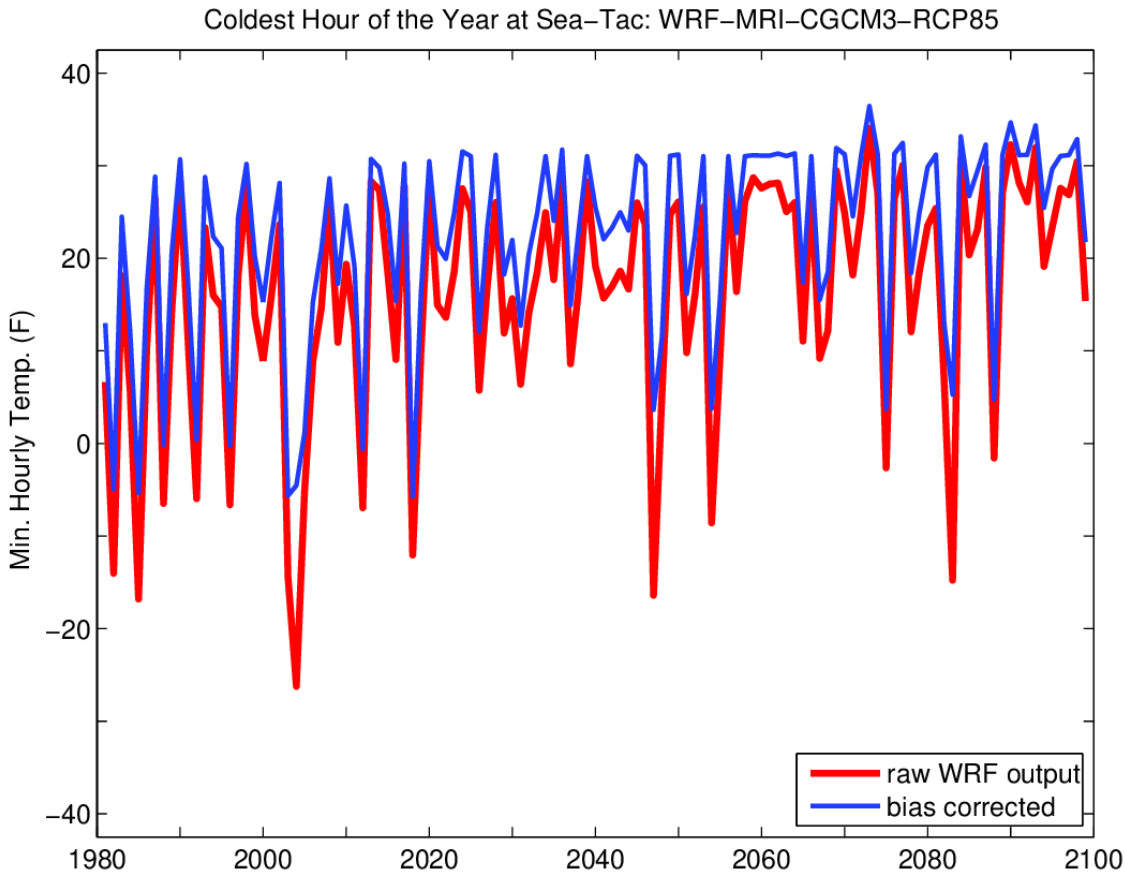

Figure A12. Time series of annual minimum temperature for MRI CGCM3, RCP 8.5.

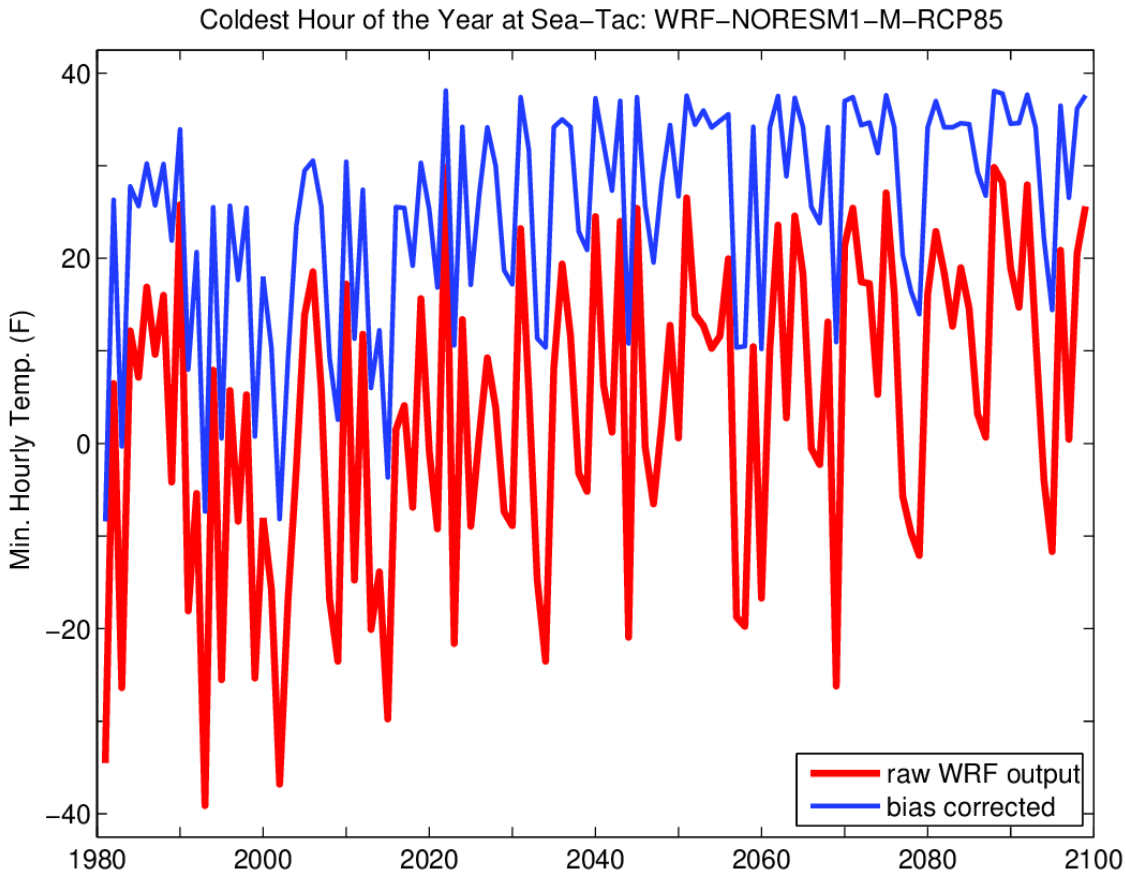

Figure A13. Time series of annual minimum temperature for NorESM1-M, RCP 8.5.